

## Supporting Information

### Generalized syntheses of nanocrystal/graphene hybrids in high-boiling-point organic solvents

Danny Wei-Ping Pang,<sup>‡</sup> Fang-Wei Yuan,<sup>‡</sup> Yan-Cheng Chang, Guo-An Li and  
Hsing-Yu Tuan\*

Department of Chemical Engineering, National Tsing Hua University, Hsinchu, Taiwan  
30013, R.O.C.

## Table of Contents

<b>Table S1.</b> Detail experimental parameters.....	S3
<b>Figure S1.</b> AFM images of GO.....	S4
<b>Figure S2.</b> TEM image of GO.....	S5
<b>Figure S3.</b> XRD patterns of graphite, graphite oxide and OLA-GO.....	S6
<b>Figure S4.</b> FTIR spectra of GO, OLA-GO and OLA.....	S7
<b>Figure S5.</b> XPS spectra of GO and OLA-GO.....	S8
<b>Figure S6.</b> LRTEM and HRTEM images of NC/CCG hybrids.....	S9
<b>Figure S7.</b> HR-XPS analyses of NC/CCG hybrids.....	S25
<b>Figure S8.</b> XRD spectra of Pt nanocrystals synthesized with and without OLA-GO...	S33

**Table S1** Detail experimental parameters of all the NC/CCG hybrids.

NCs	HU/HI	Precursors/Solvents in 3-neck flask	Inj. Shot	Inj. Temp.	Rxn. Temp.	Inert /Open	Rxn. Time
Cu	HI	Oleylamine	0.1 mmol of Cu(acac) <sub>2</sub> + OLA-GO + 1 ml oleylamine, heated to 100°C to form complex	260°C	260°C	Inert	30 mins
Ag	HU	0.5 mmol AgNO <sub>3</sub> + 15 ml Toluene + OLA-GO	-	-	110°C (10°C/min)	Inert	6 hrs
Pd	HU	1.64 mmol Pd(acac) <sub>2</sub> + 10 ml TOP + OLA-GO	-	-	300°C (5°C/min)	Inert	30 mins
Pt	HU	0.05 mmol Pt(acac) <sub>2</sub> + OLA-GO + 10 ml Benzyl Ether	-	-	230°C (10°C/min)	Inert	1 hr
Fe <sub>3</sub> O <sub>4</sub>	HU	0.03 mmol Fe(acac) <sub>3</sub> + 5 ml Benzyl Ether + OLA-GO	-	-	300°C (20°C/min)	Inert	1 hr
Fe <sub>2</sub> O <sub>3</sub>	HI	0.09 g Oleic acid + 10 ml diphenyl ether	0.15 mmol of Fe(CO) <sub>5</sub> + OLA-GO	100°C	265°C (5°C/min)	Inert	1 hr
CdS	HI	0.1 mmol CdO + 0.08 g Oleic Acid + 4.9 ml n-Octadecene	0.05 mmol Sulfur powder + 1 ml n-Octadecene + OLA-GO	300°C	250°C	Inert	30 mins
CdSe	HI	0.1 mmol CdO + 0.5 g Oleic Acid + 10 ml of n-Octadecene	1ml of (0.37mmol Selenium powder + 5ml n-Octadecene + 0.4ml TOP)	225°C	225°C	Inert	30 mins
CdTe	HI	0.1 mmol of CdO + 0.09 g Oleic Acid + 4.8 ml ODE	0.05 mmol of Tellurium powder + 1.2 ml TOP + OLA-GO, heat up to 200°C to form complex, drop to room temperature before injection	220°C	190°C	Inert	30 mins
CuInS <sub>2</sub>	HI	0.1 mmol Cu(acac) <sub>2</sub> + 0.1 mmol In(acac) <sub>3</sub> + 7 ml ortho-Dichlorobenzene	0.02 mmol of Sulfur powder + OLA-GO + 3 ml ortho-Dichlorobenzene	100°C	185°C (20°C/min)	Inert	1 hr
CuInSe <sub>2</sub>	HU	0.1 mmol CuCl + 0.1 mmol InCl <sub>3</sub> + 0.2 mmol Se + OLA-GO	-	-	240°C (3°C/min)	Inert	4 hrs
In <sub>2</sub> O <sub>3</sub>	HU	0.1 mmol In(acac) <sub>3</sub> + OLA-GO + 10ml Benzyl Ether	-	-	300°C	Open	1 hr
SnO <sub>2</sub>	HU	0.1mmol SnCl <sub>2</sub> (acac) <sub>2</sub> + OLA-GO + 10ml Benzyl Ether	-	-	280°C	Open	1 hr
Ru	HU	0.06 mol Ru(acac) <sub>3</sub> + 0.12 mmol of 1,2 Hexadecanediol + OLA-GO + 10 ml Benzyl Ether	-	-	300°C (8°C/min)	Inert	30 mins
ZnS	HU	1.79 g Oleic acid + 3 ml n-Octadecene + 3 mmol Sulfur Powder + 0.5 ml Diethylzinc	-	-	300°C (5°C/min)	Inert	2 hrs
ZnSe	HI	7.5 ml Hexadecylamine	0.4 ml Ditethylzinc + 0.5 ml of 1 M TOP-Se complex + 4 ml TOP + OLA-GO	310°C	270°C	Inert	1 hr

\*Note: **HU**: Heating up; **HI**: Hot injection; **Inj.**: Injection; **Temp.**: Temperature; **Rxn.**: Reaction; **acac**: Acetylacetone; **TOP**: Trioctylphosphine.

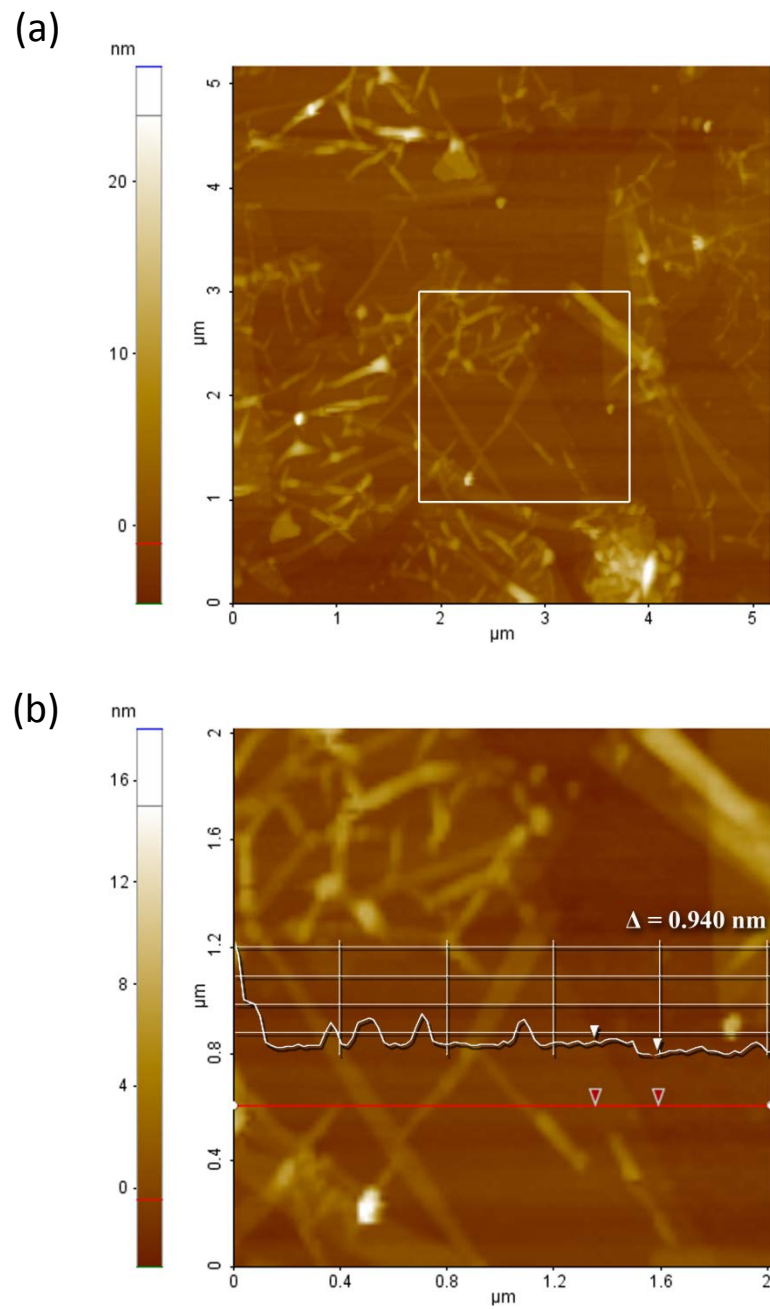


**Fig. S1** AFM images of (a) GO. (b) Height profile of the square cropped-area of (a). Height difference measured between the GO sheet and substrate (the cursor pair in b) is 0.940 nm, consistent with the thickness of single layer GO sheet.

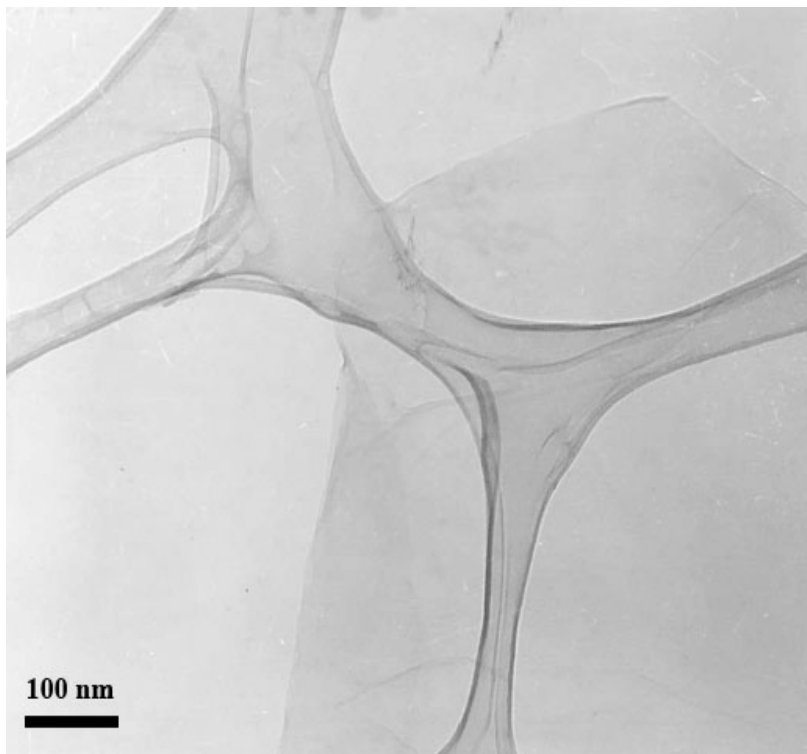


**Fig. S2** TEM image of as-prepared GO on holey carbon support film. The crumpled silk wave is the landmark of thin graphene sheet.

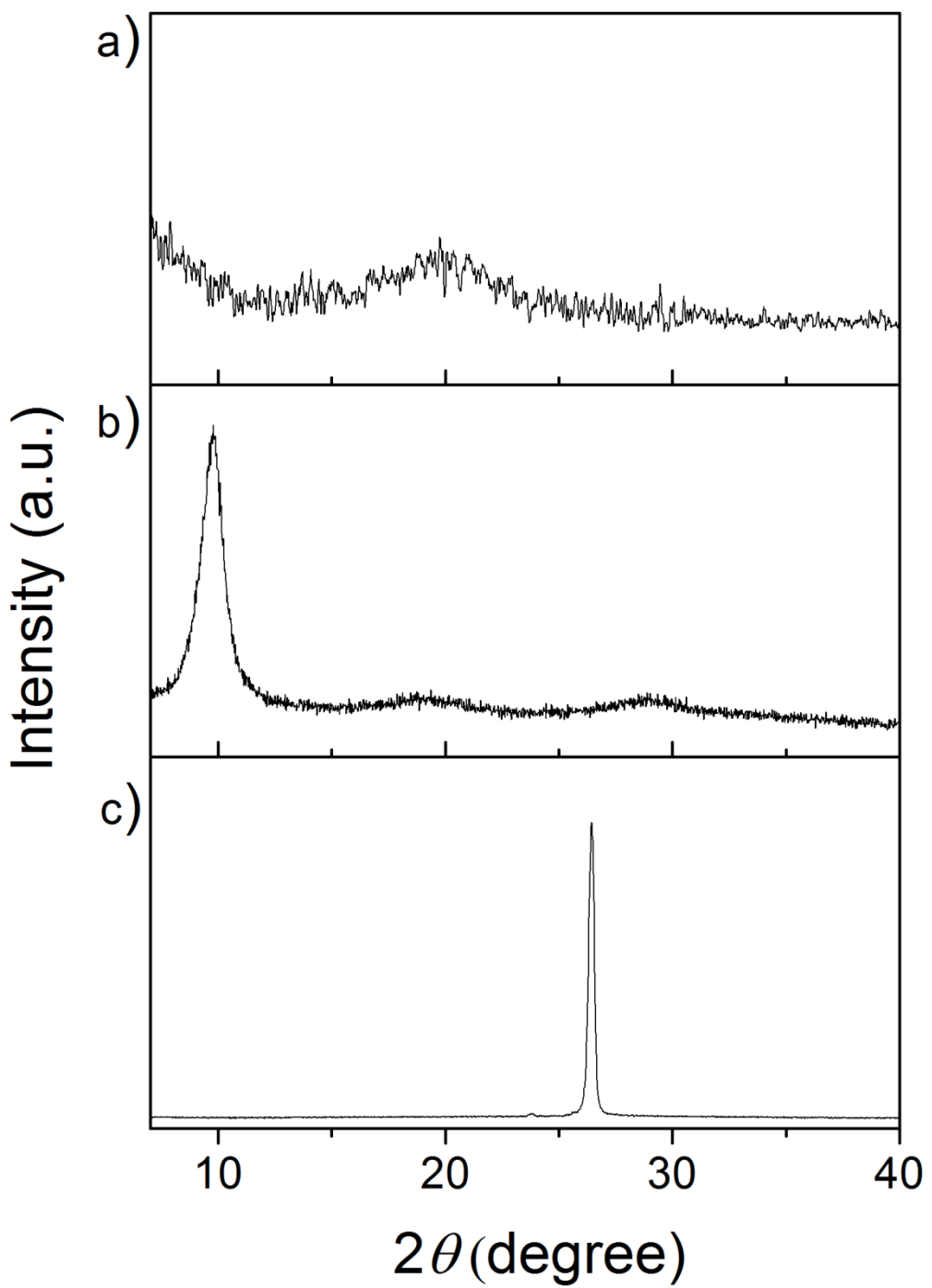


**Fig. S3** XRD patterns of (a) OLA-GO, (b) graphite oxide and (c) graphite.

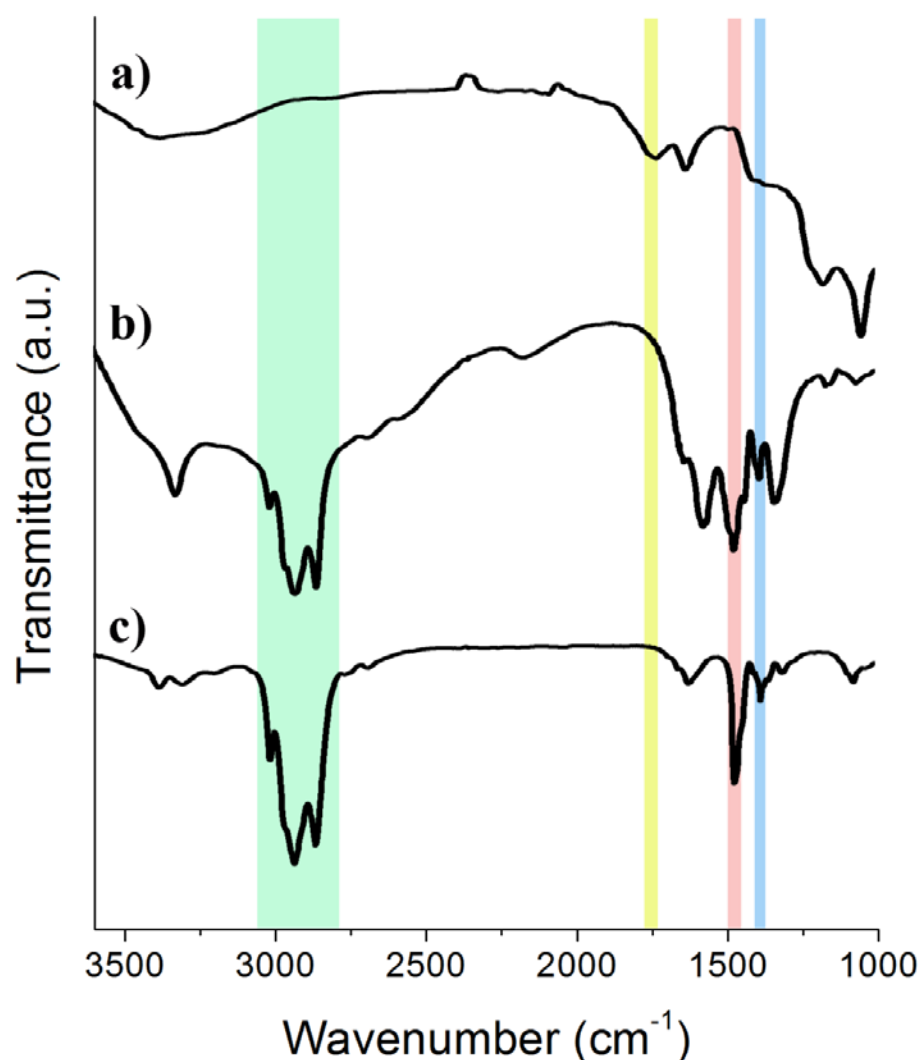


**Fig. S4** FTIR spectra of (a) GO, (b) OLA-GO, and (c) OLA. The bands located at  $2850\text{cm}^{-1}$  and  $2925\text{cm}^{-1}$  in (b) and (c) corresponded to anti-symmetric and symmetric C-H stretching vibrations of OLA alkyl group respectively. The bands at  $1460\text{cm}^{-1}$  and  $1380\text{cm}^{-1}$  are C-H bending vibrations of alkyl groups. The band  $1730\text{cm}^{-1}$ , which is assigned to -COOH vibrations of GO is disappeared after functionalization, as shown in (a) and (b).

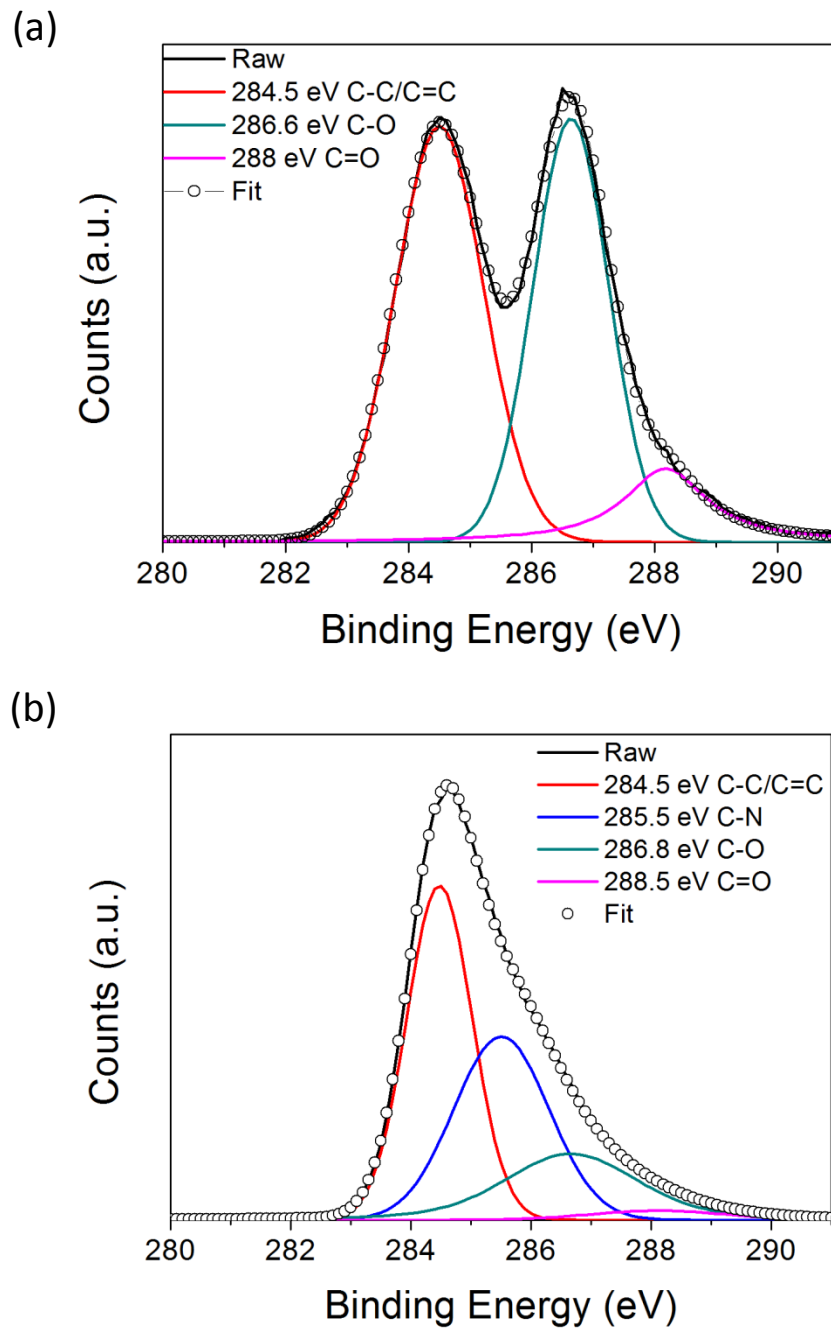


**Fig. S5** XPS spectra of (a) as-prepared GO, and (b) OLA-GO.

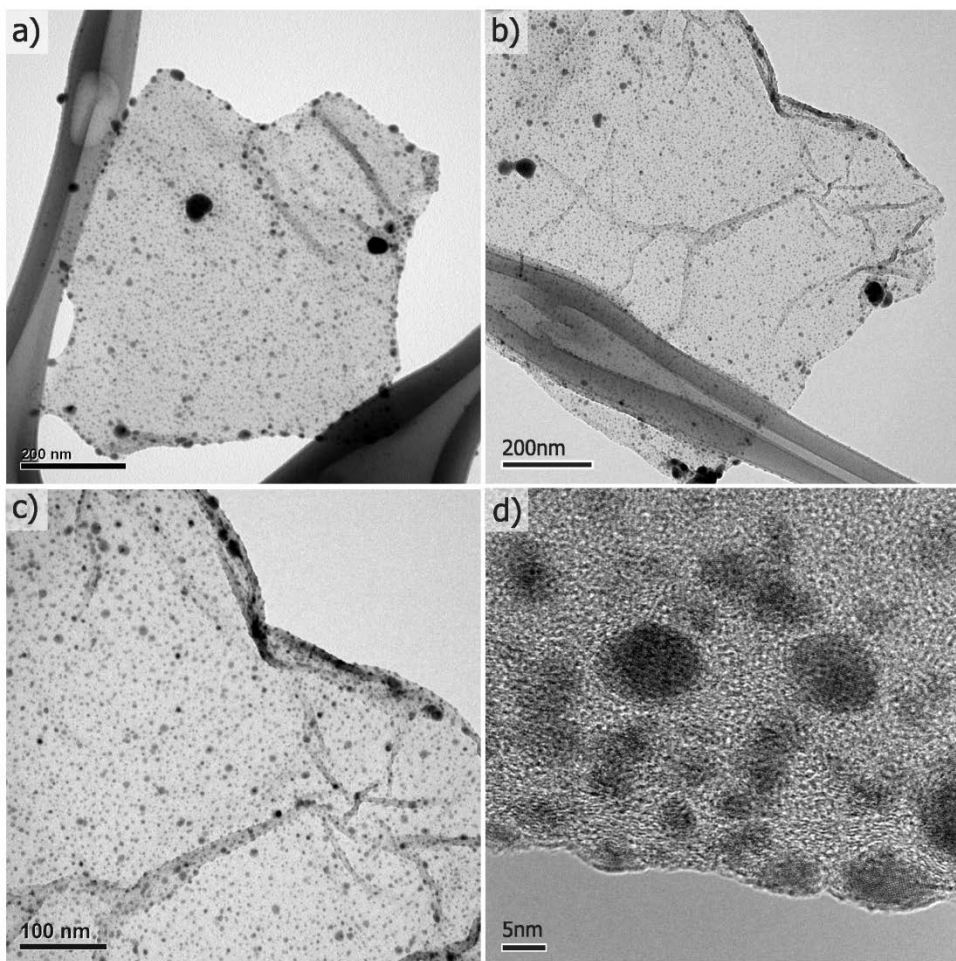


**Fig. S6-1** (a-d) TEM images of Ag/CCG hybrid.

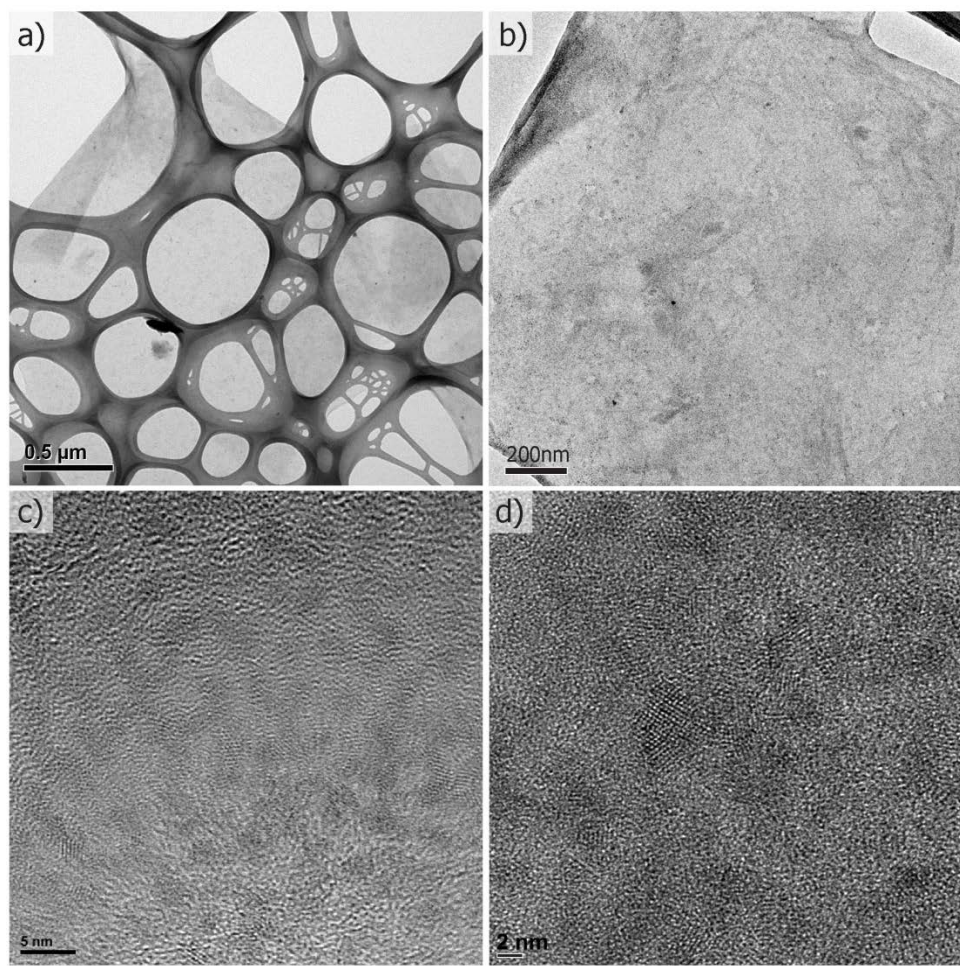


**Fig. S6-2** (a-d) TEM images of CdS/CCG hybrid.

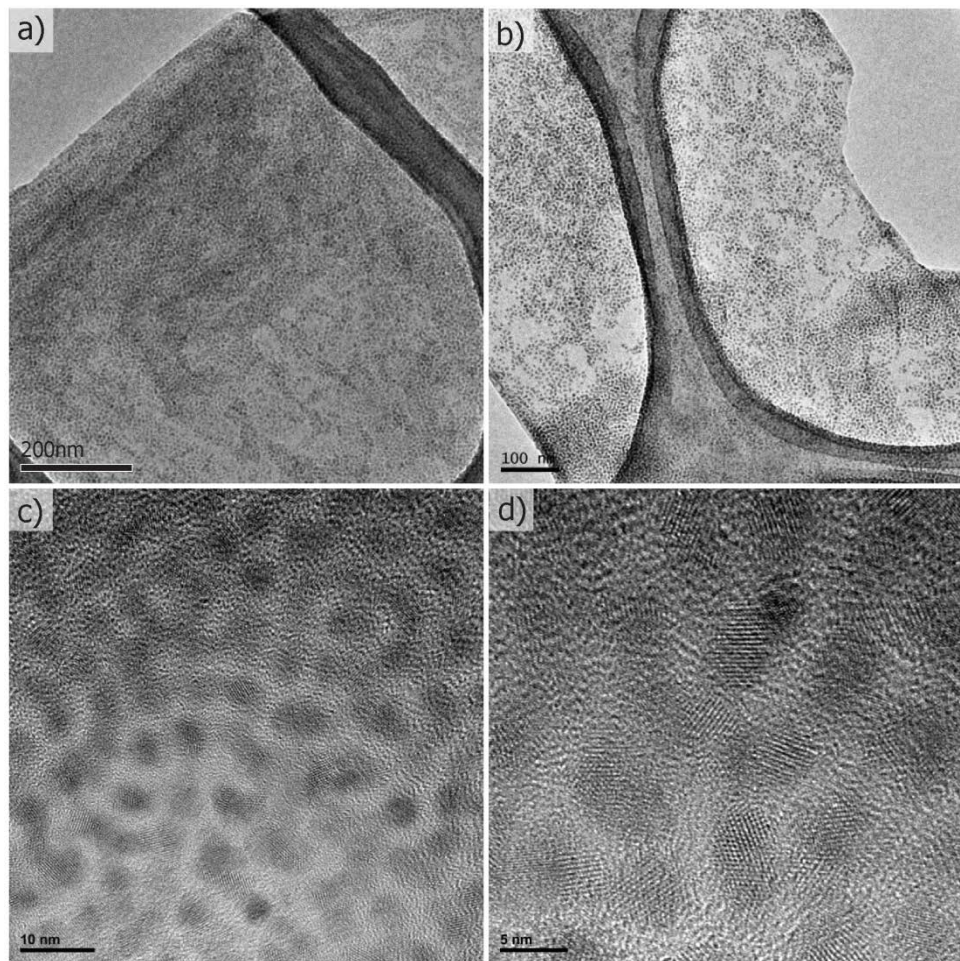


**Fig. S6-3** (a-d) TEM images of CdSe/CCG hybrid.

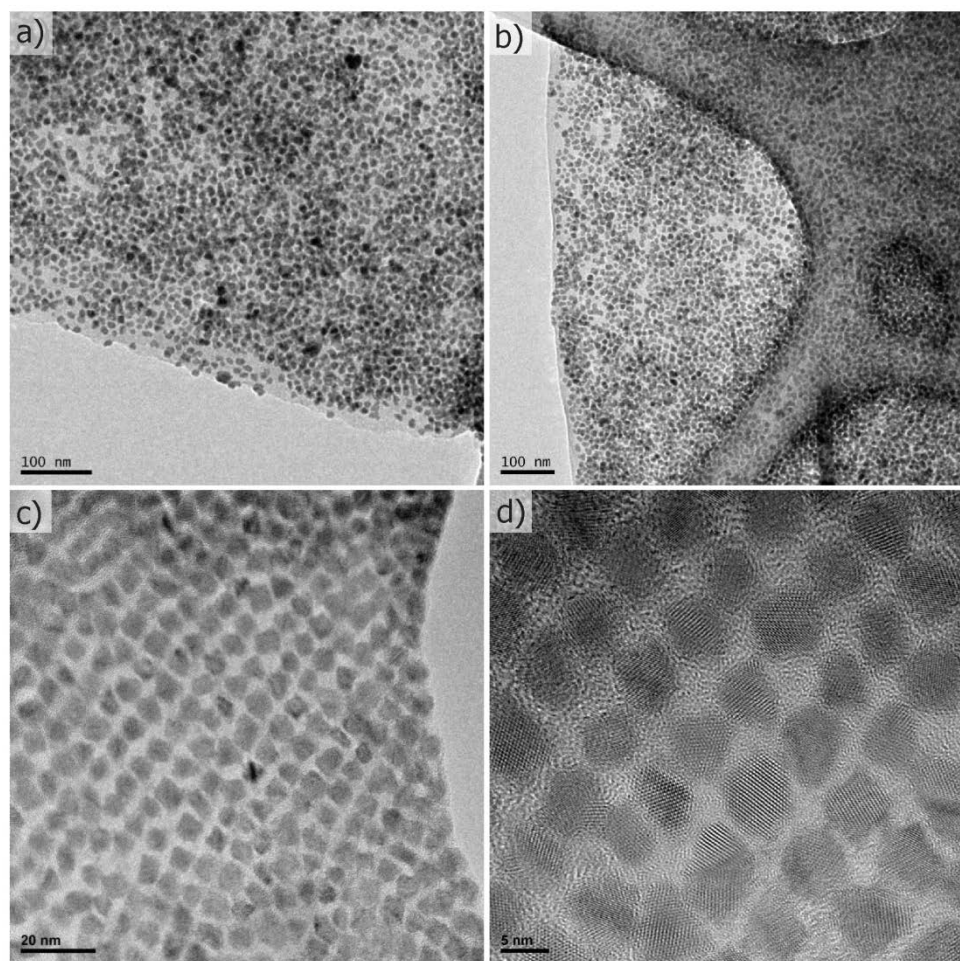


**Fig. S6-4** (a-d) TEM images of CdTe/CCG hybrid.

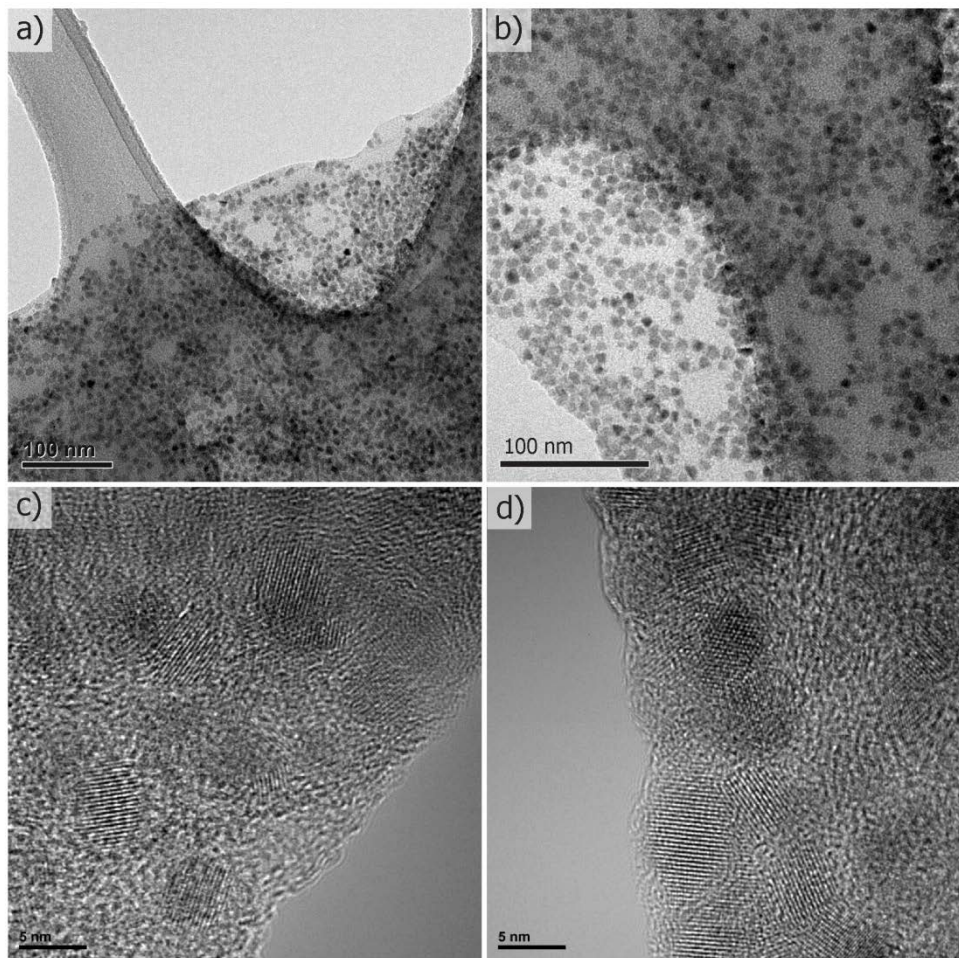


**Fig. S6-5** (a-d) TEM images of CuInS<sub>2</sub>/CCG hybrid.

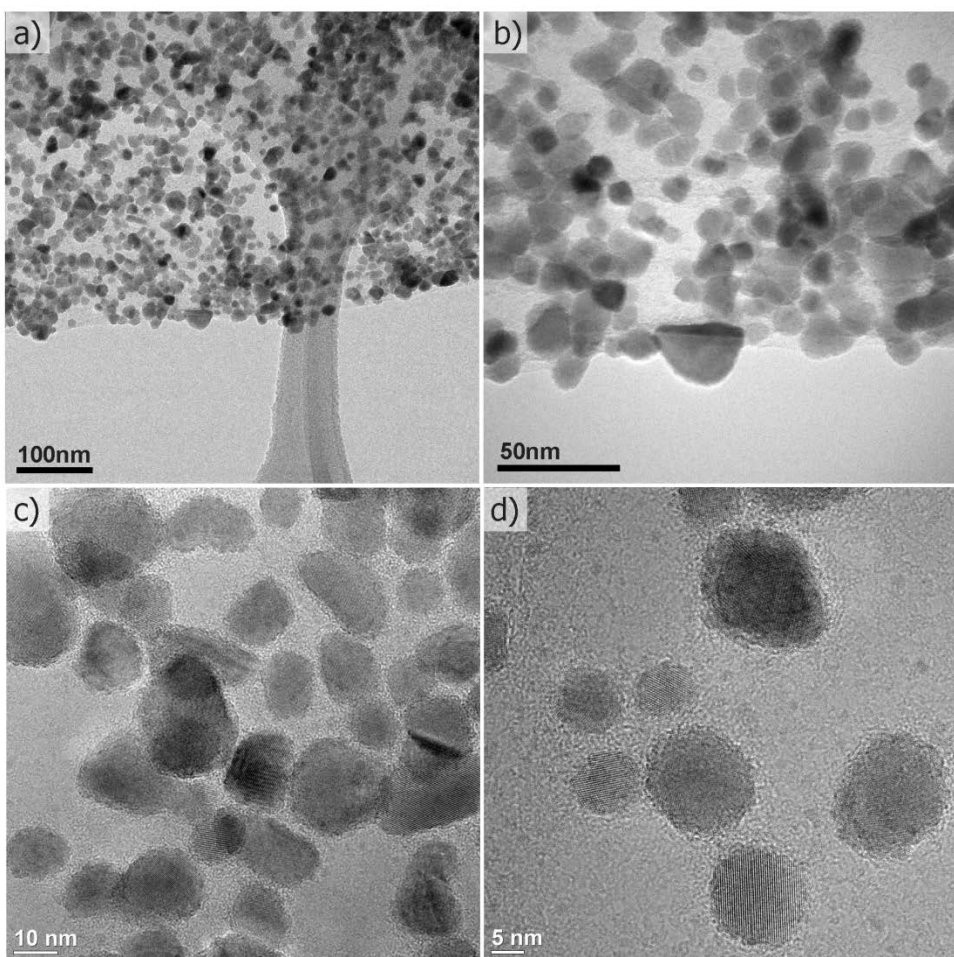


**Fig. S6-6** (a-d) TEM images of CuInSe<sub>2</sub>/CCG hybrid.

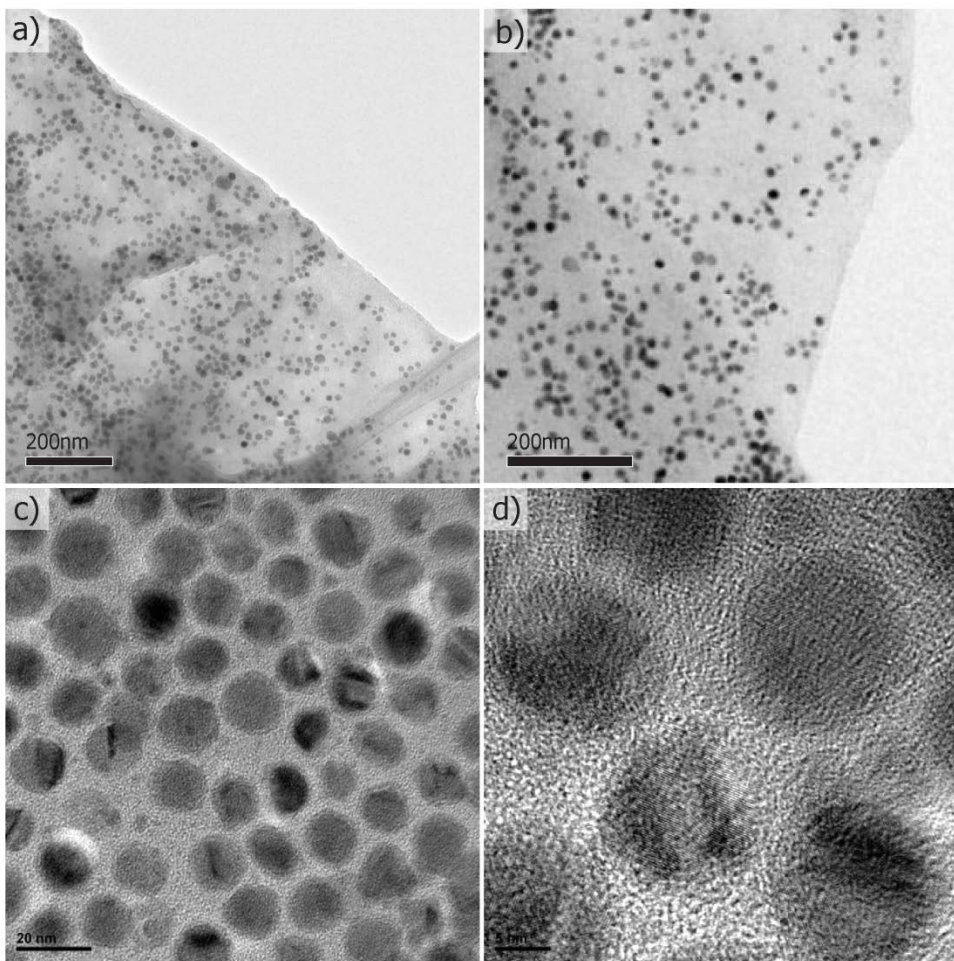


**Fig. S6-7** (a-d) TEM images of Cu/CCG hybrid.

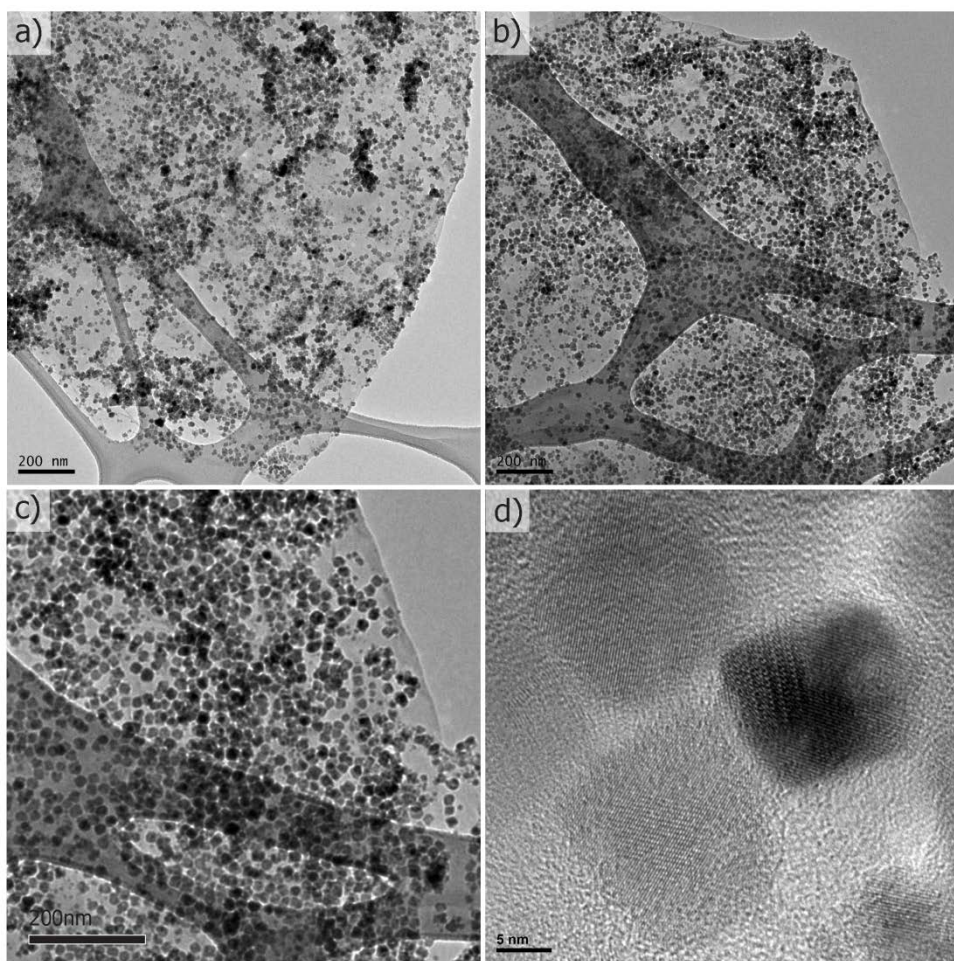


**Fig. S6-8** (a-d) TEM images of Fe<sub>2</sub>O<sub>3</sub>/CCG hybrid.

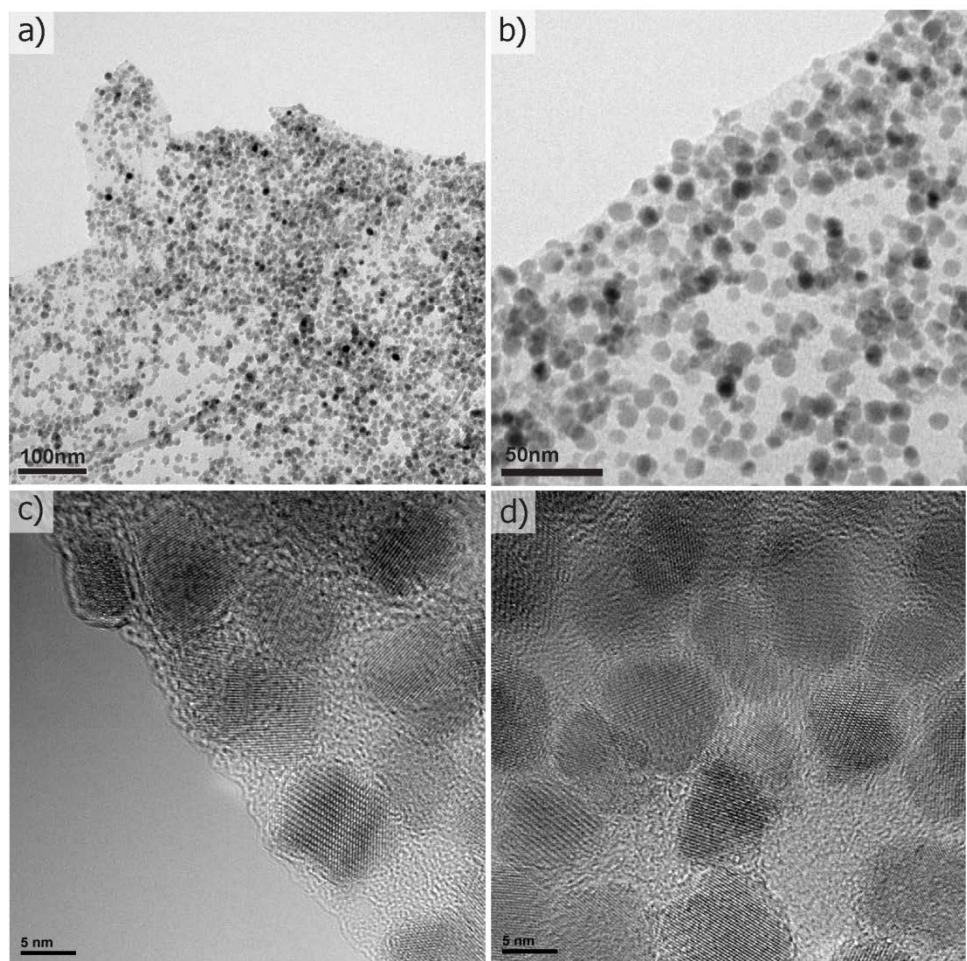


**Fig. S6-9** (a-d) TEM images of Fe<sub>3</sub>O<sub>4</sub>/CCG hybrid.

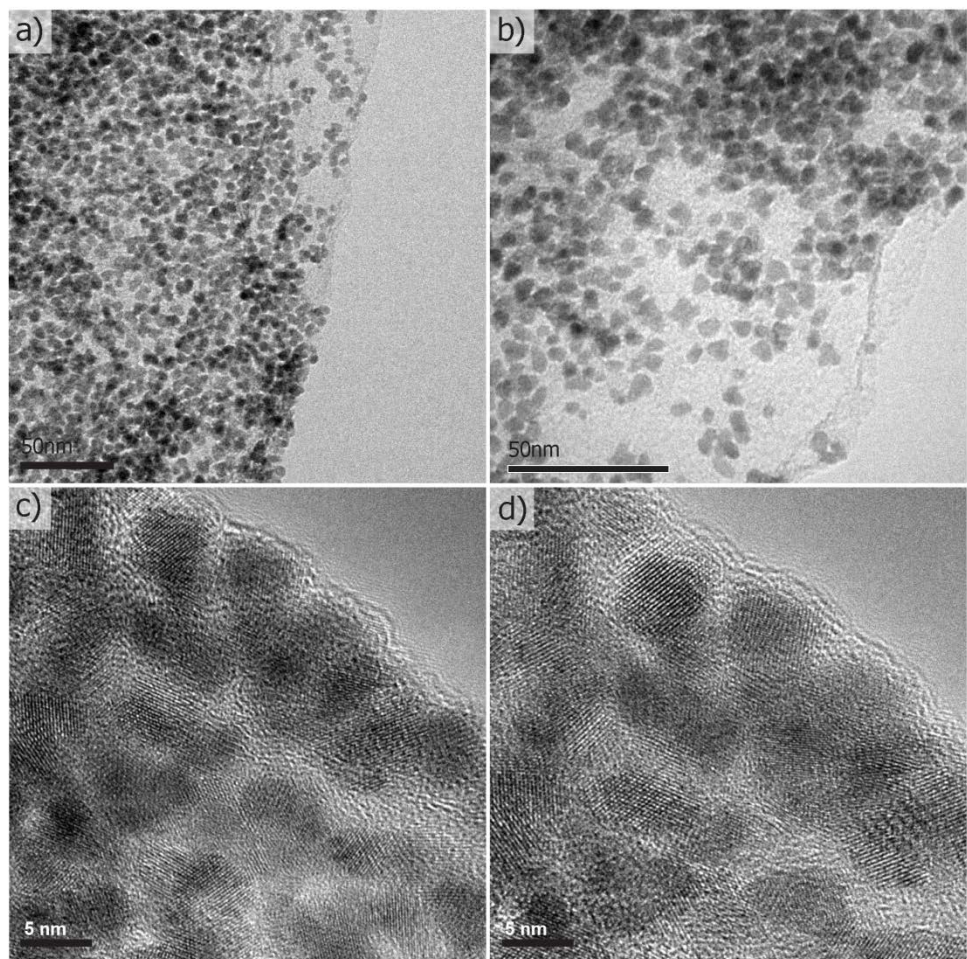


**Fig. S6-10** (a-d) TEM images of  $\text{In}_2\text{O}_3/\text{CCG}$  hybrid.

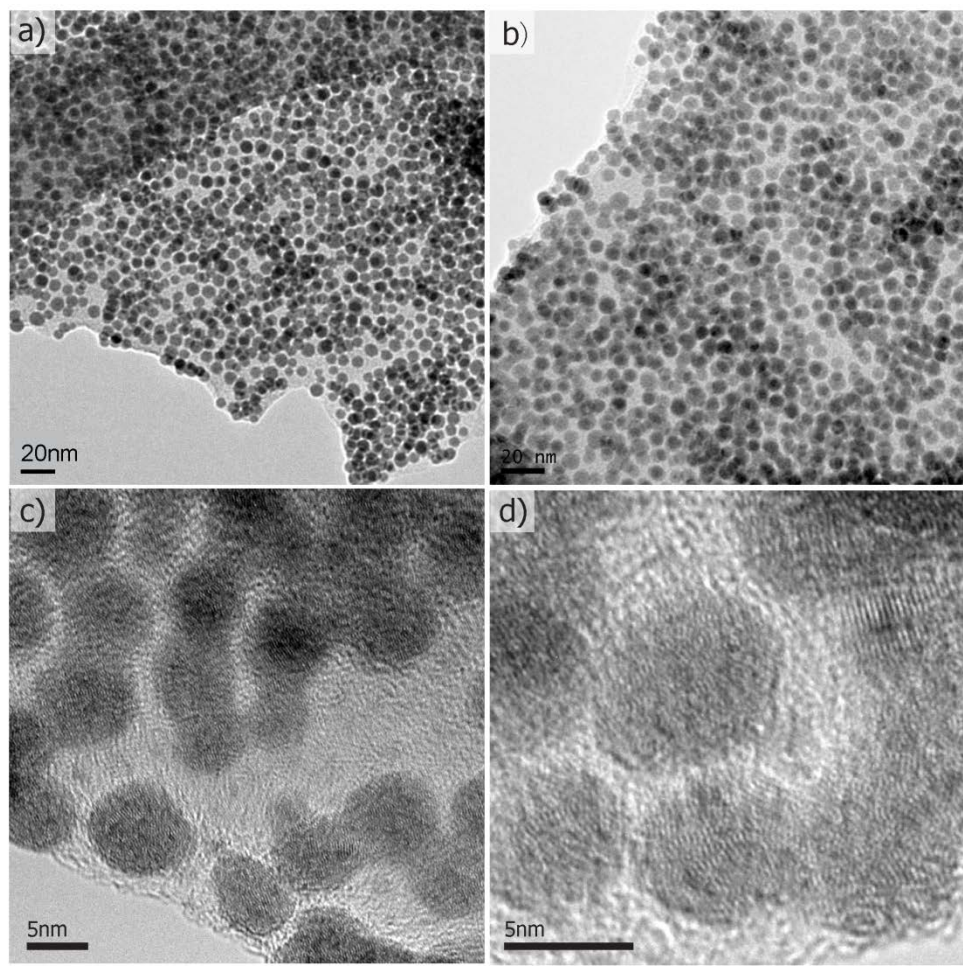


**Fig. S6-11** (a-d) TEM images of Pd/CCG hybrid.

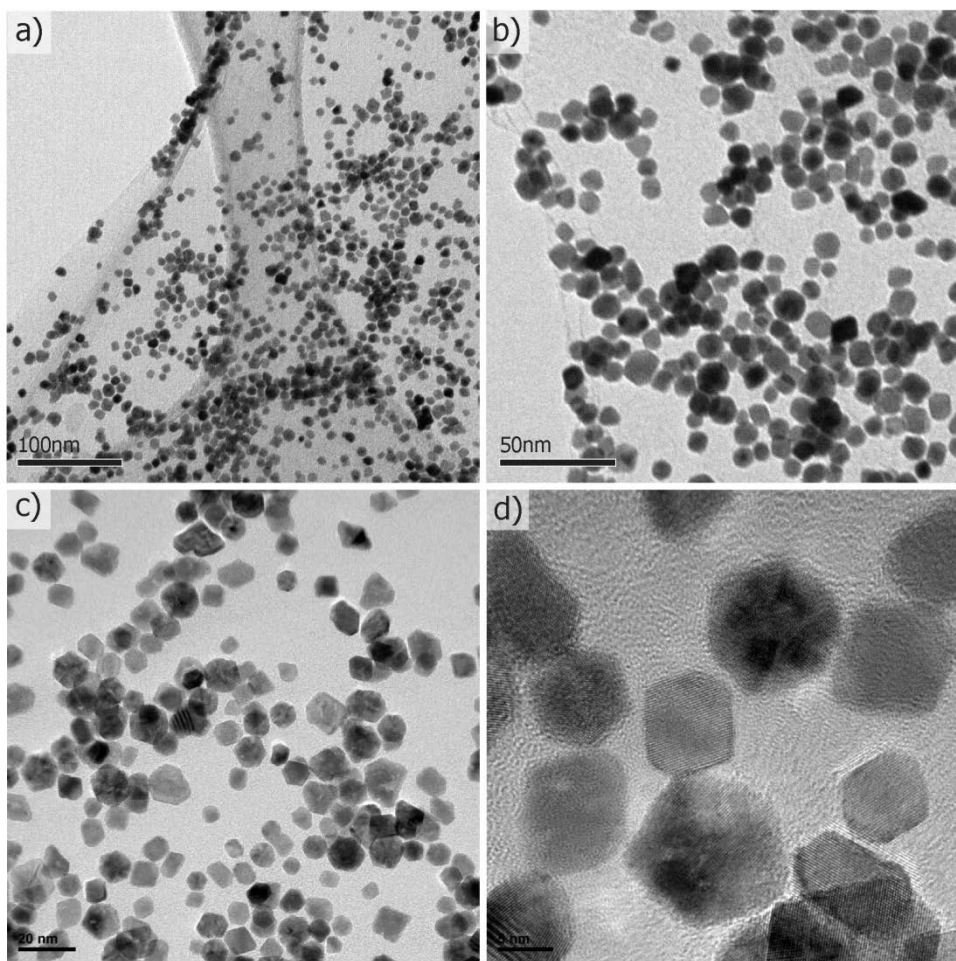


**Fig. S6-12** (a-d) TEM images of Pt/CCG hybrid.

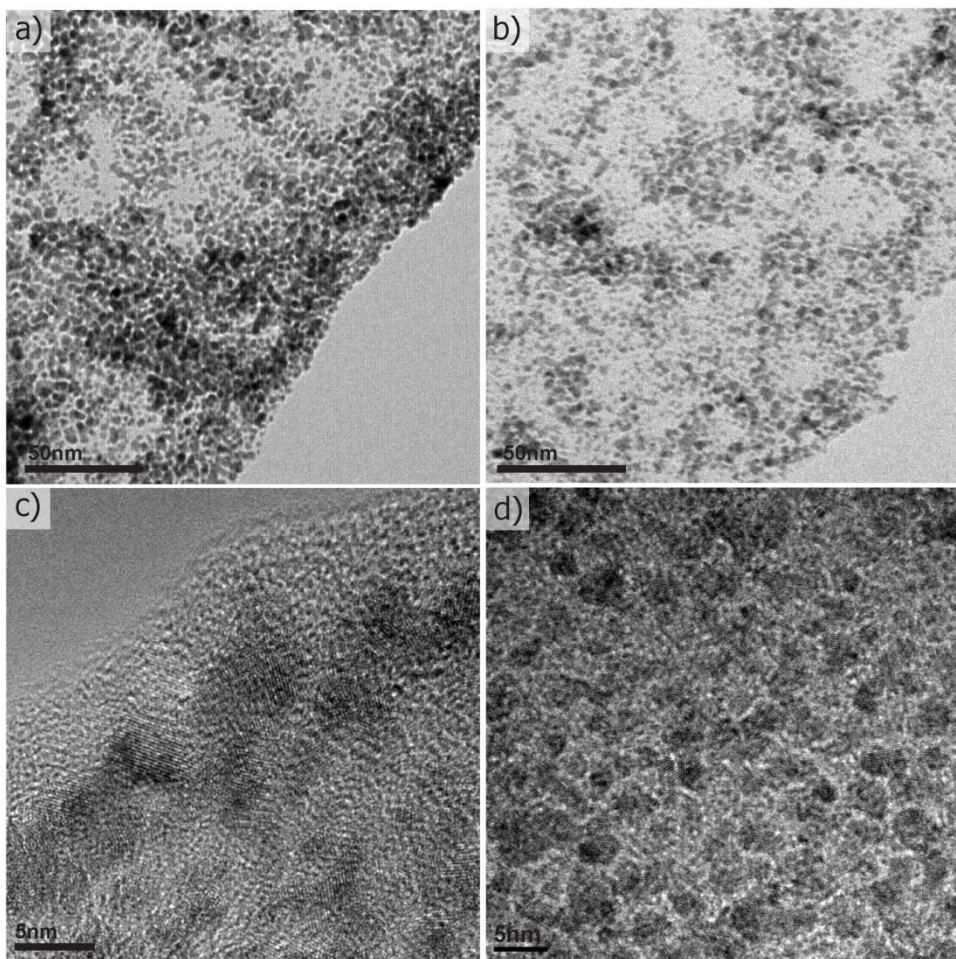


**Fig. S6-13** (a-d) TEM images of Ru/CCG hybrid.

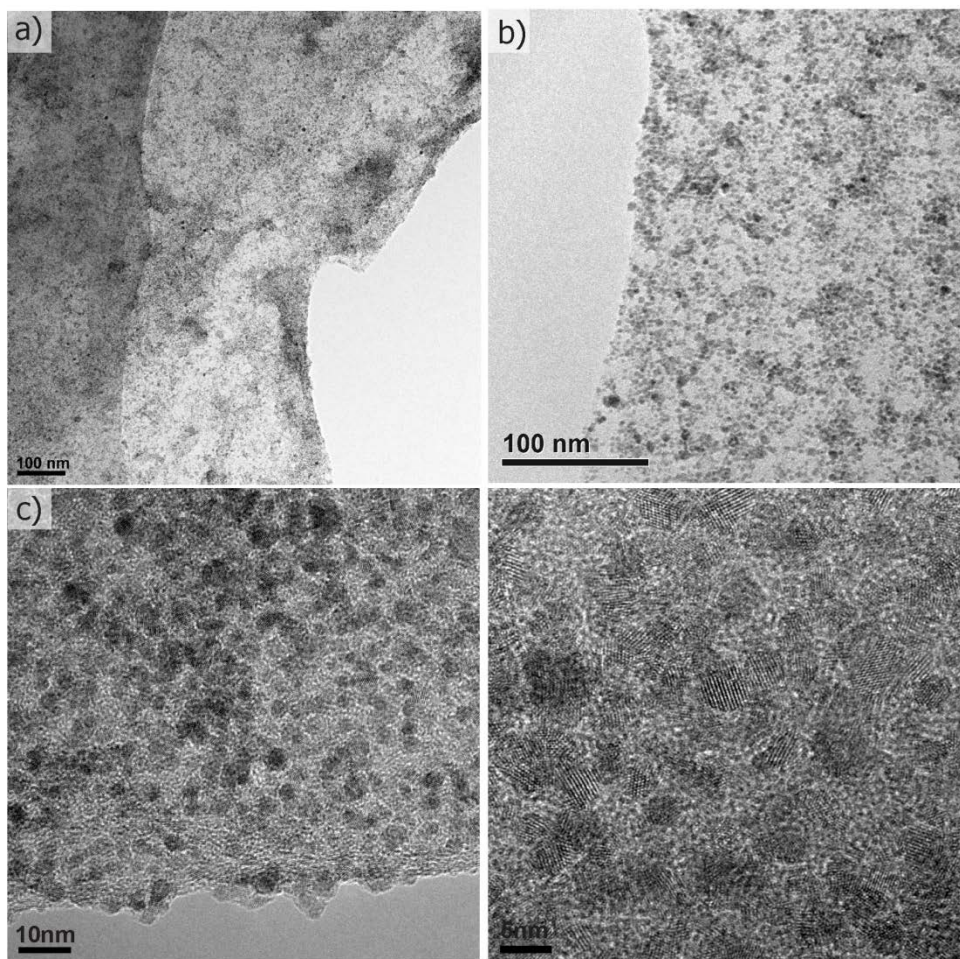


**Fig. S6-14** (a-d) TEM images of  $\text{SnO}_2/\text{CCG}$  hybrid.

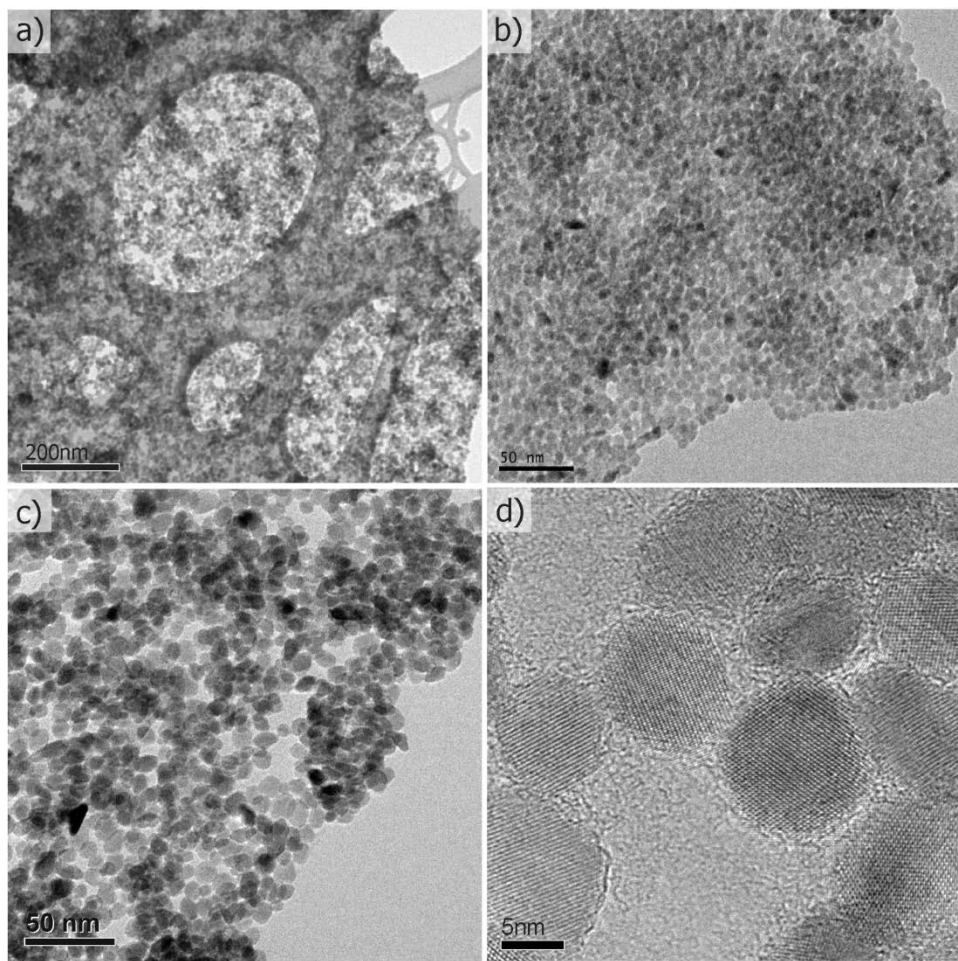


**Fig. S6-15** (a-d) TEM images of ZnS/CCG hybrid.

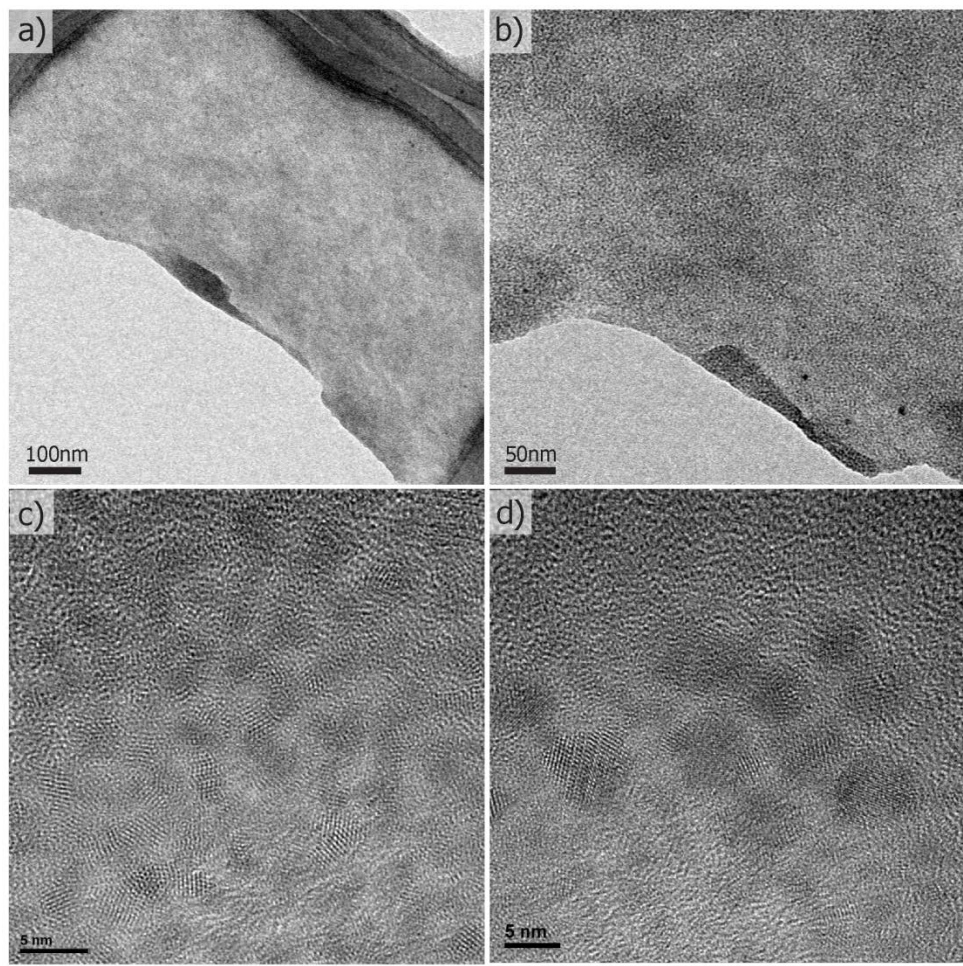


**Fig. S6-16** (a-d) TEM images of ZnSe/CCG hybrid.

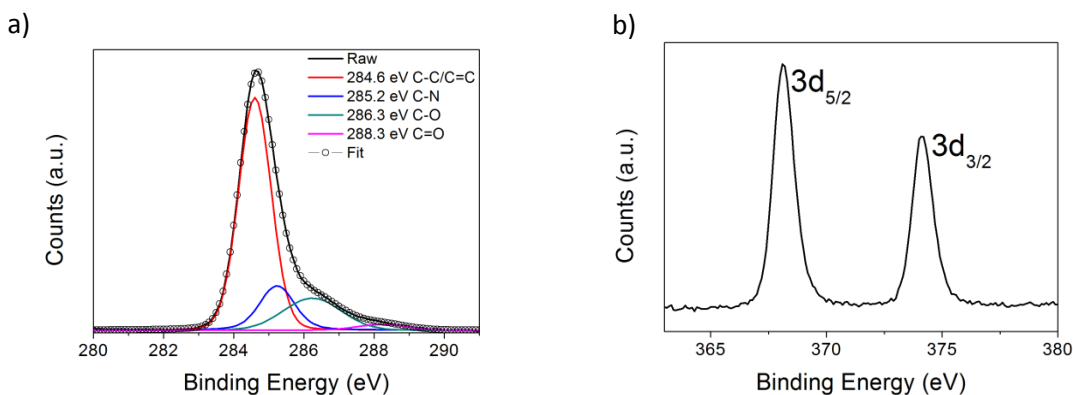


**Fig. S7-1** HR-XPS analyses of Ag/CCG hybrid. a) C 1s and b) Ag 3d core level spectrum.

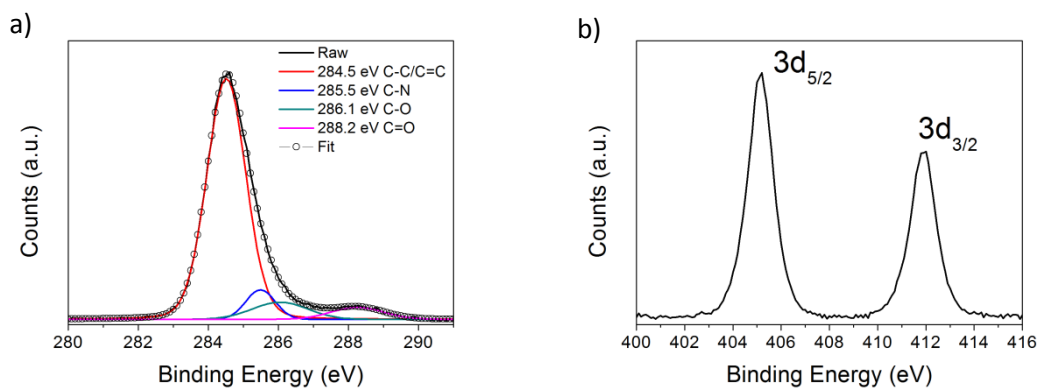


**Fig. S7-2** HR-XPS analyses of CdS/CCG hybrid. a) C 1s and b) Cd 3d core level spectrum.

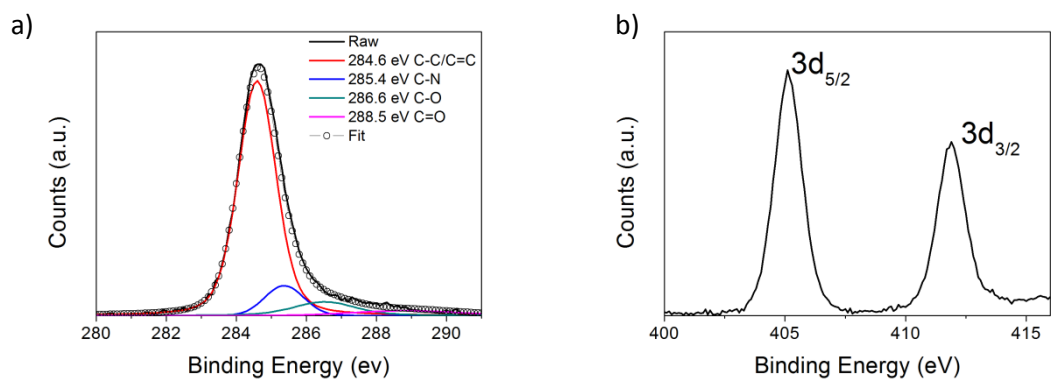


**Fig. S7-3** HR-XPS analyses of CdSe/CCG hybrid. a) C 1s and b) Cd 3d core level spectrum.

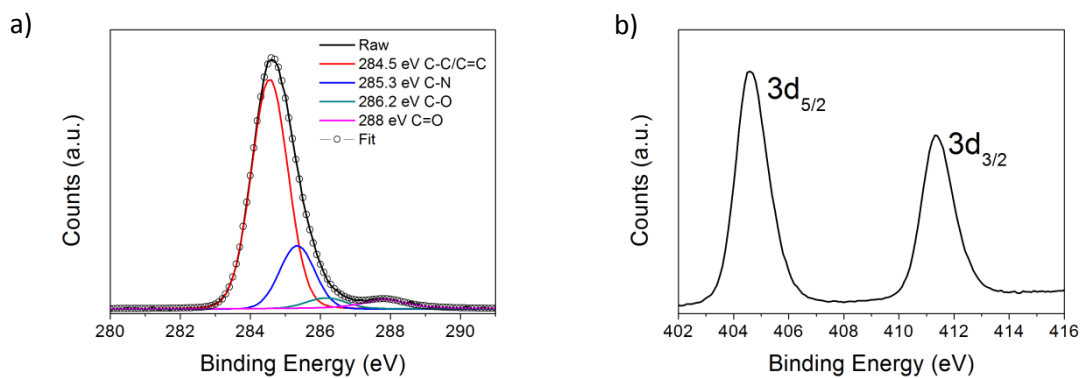


**Fig. S7-4** HR-XPS analyses of CdTe/CCG hybrid. a) C 1s and b) Cd 3d core level spectrum.

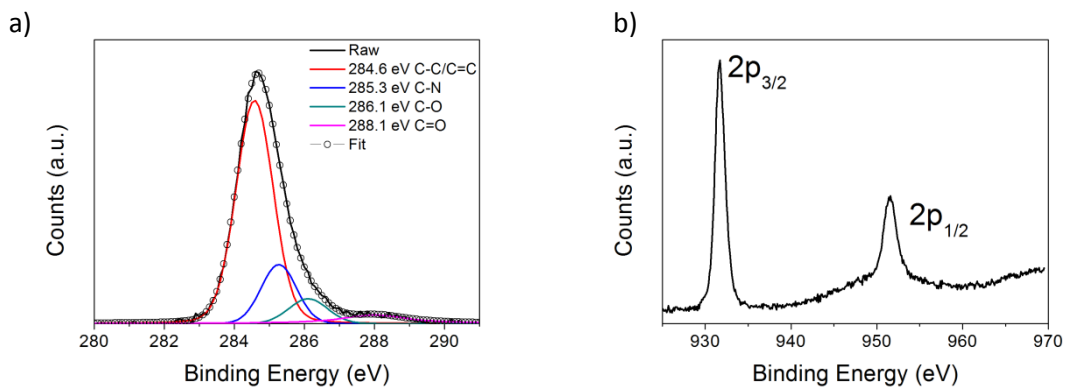


**Fig. S7-5** HR-XPS analyses of CuInS<sub>2</sub>/CCG hybrid. a) C 1s and b) Cu 2p core level spectrum.

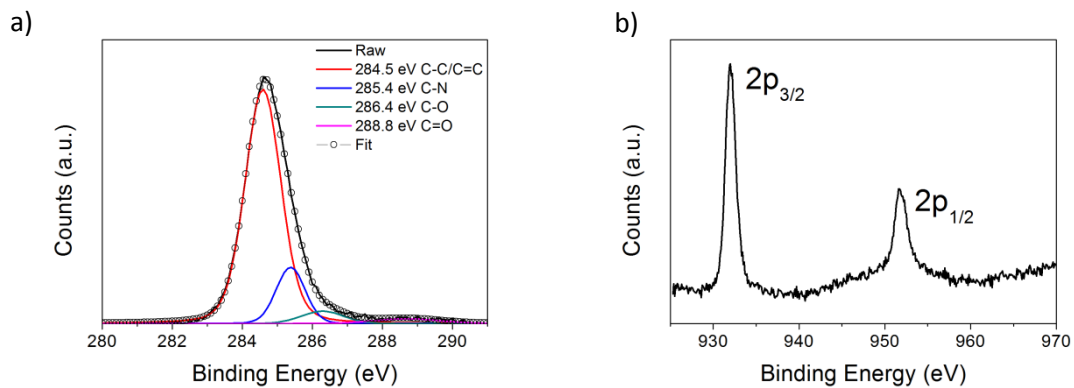


**Fig. S7-6** HR-XPS analyses of CuInSe<sub>2</sub>/CCG hybrid. a) C 1s and b) Cu 2p core level spectrum.

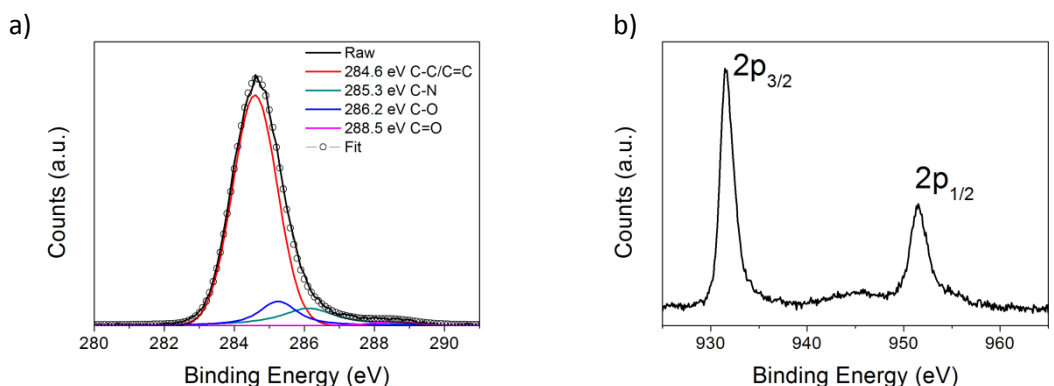


**Fig. S7-7** HR-XPS analyses of Cu/CCG hybrid. a) C 1s and b) Cu 2p core level spectrum.

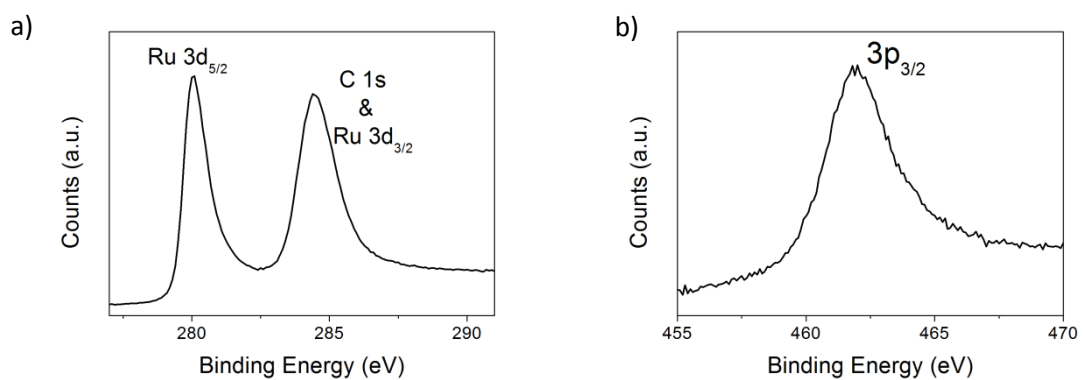


**Fig. S7-8** HR-XPS analyses of Ru/CCG hybrid. a) C 1s and b) Ru 3p core level spectrum.

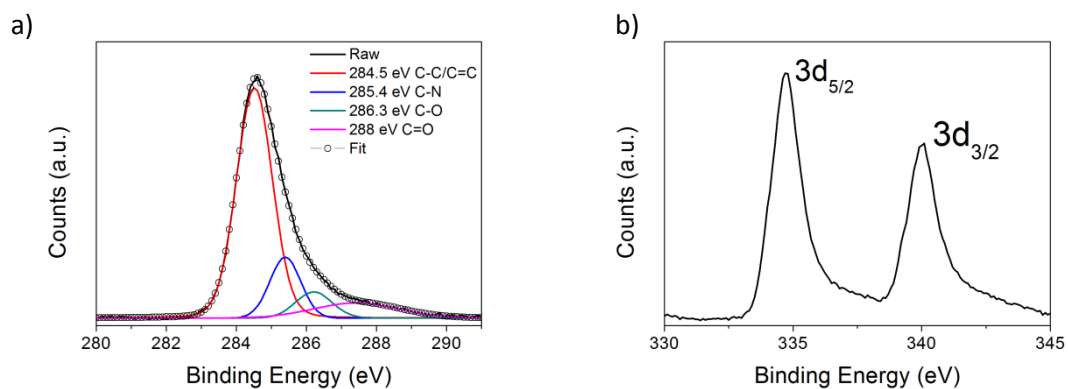


**Fig. S7-9** HR-XPS analyses of Pd/CCG hybrid. a) C 1s and b) Pd 3d core level spectrum.

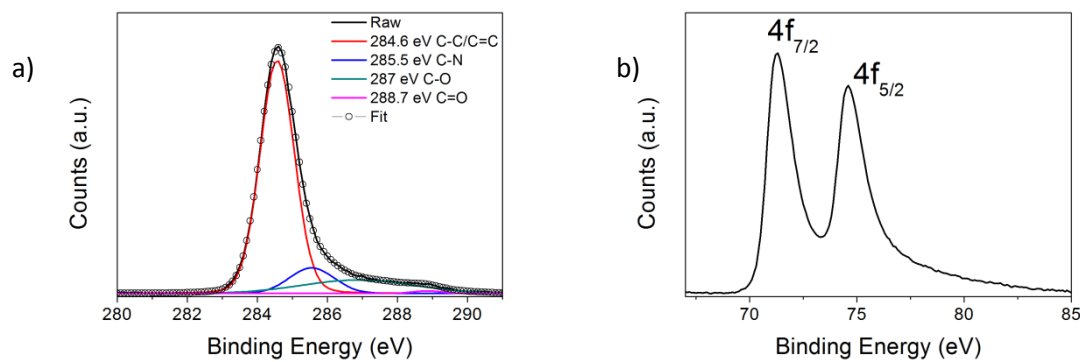


**Fig. S7-10** HR-XPS analyses of Pt/CCG hybrid. a) C 1s and b) Pt 4f core level spectrum.

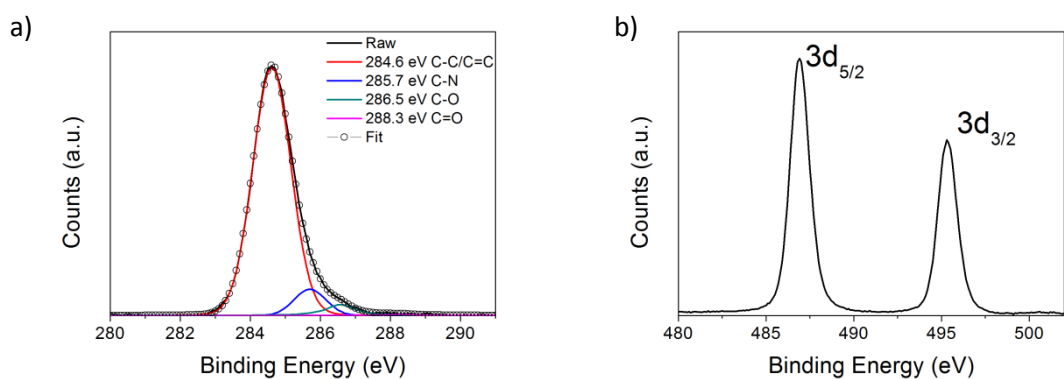


**Fig. S7-11** HR-XPS analyses of  $\text{SnO}_2/\text{CCG}$  hybrid. a) C 1s and b) Sn 3d core level spectrum.

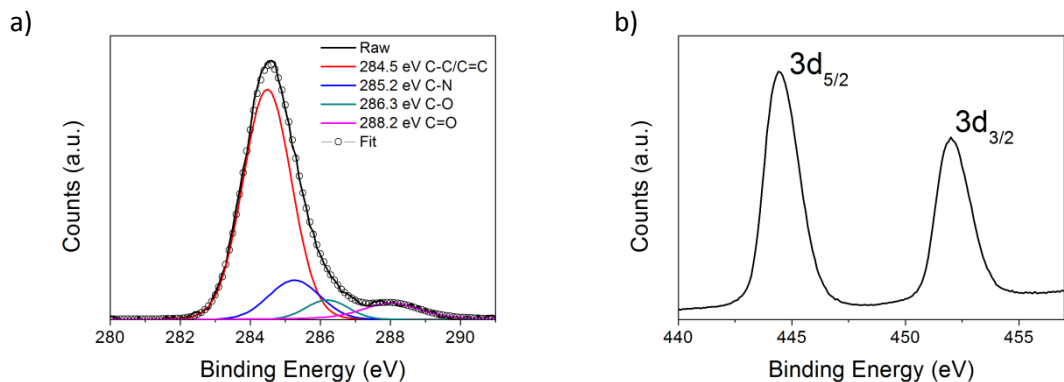


**Fig. S7-12** HR-XPS analyses of  $\text{In}_2\text{O}_3/\text{CCG}$  hybrid. a) C 1s and b) In 3d core level spectrum.

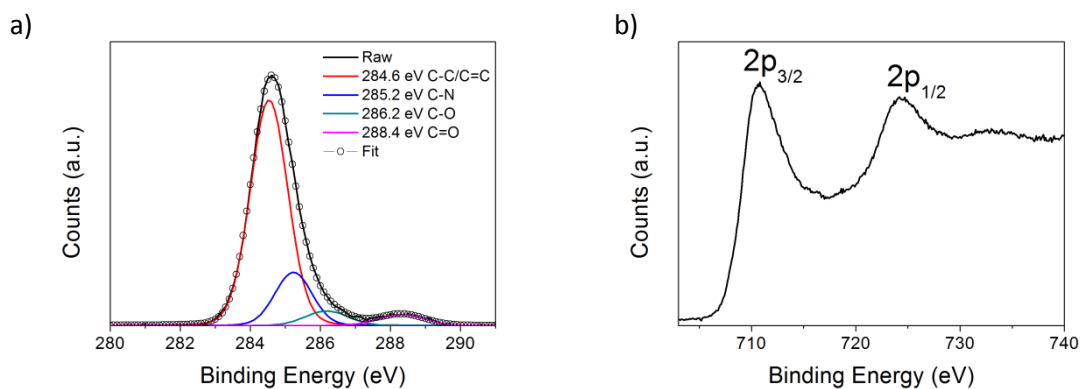


**Fig. S7-13** HR-XPS analyses of  $\text{Fe}_2\text{O}_3/\text{CCG}$  hybrid. a) C 1s and b) Fe 2p core level spectrum.

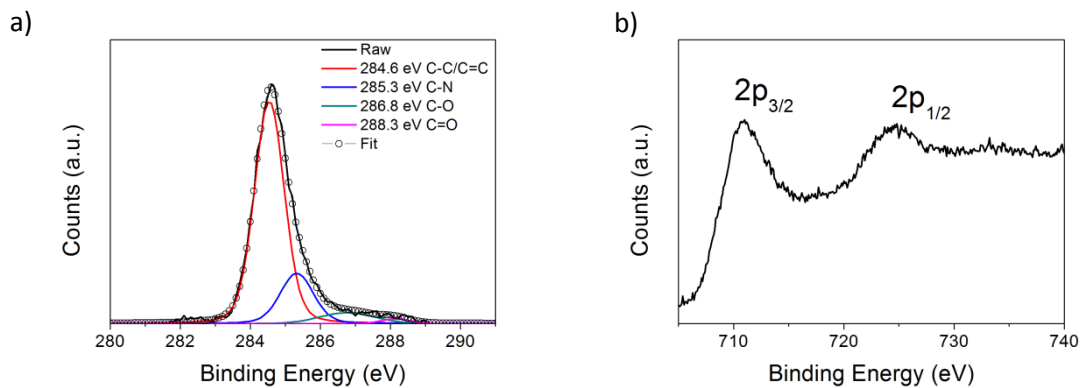


**Fig. S7-14** HR-XPS analyses of  $\text{Fe}_3\text{O}_4/\text{CCG}$  hybrid. a) C 1s and b) Fe 2p core level spectrum.

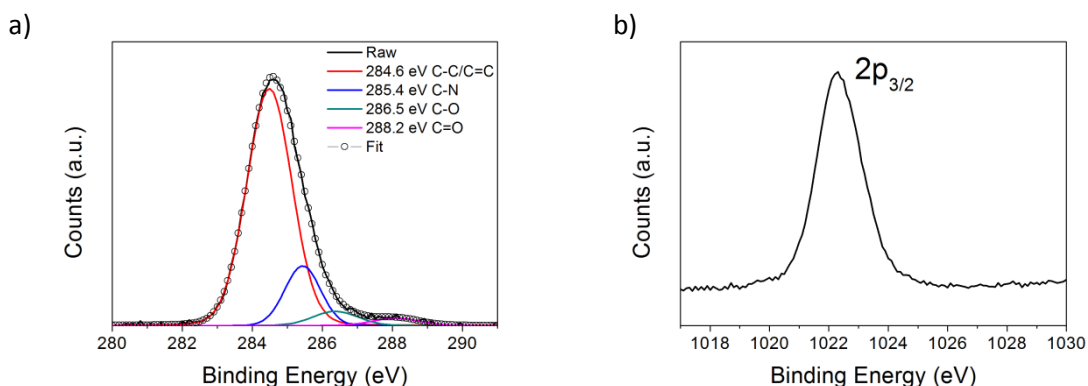


**Fig. S7-15** HR-XPS analyses of ZnS/CCG hybrid. a) C 1s and b) Zn 2p core level spectrum.

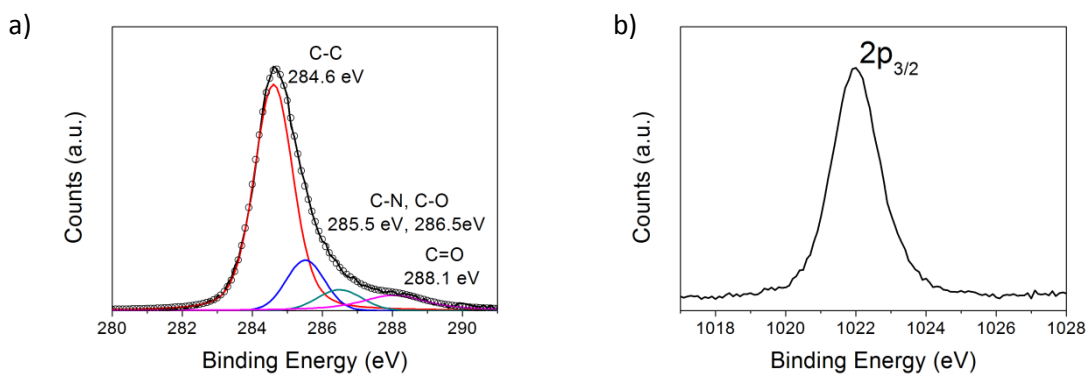


**Fig. S7-16** HR-XPS analyses of ZnSe/CCG hybrid. a) C 1s and b) Zn 2p core level spectrum.

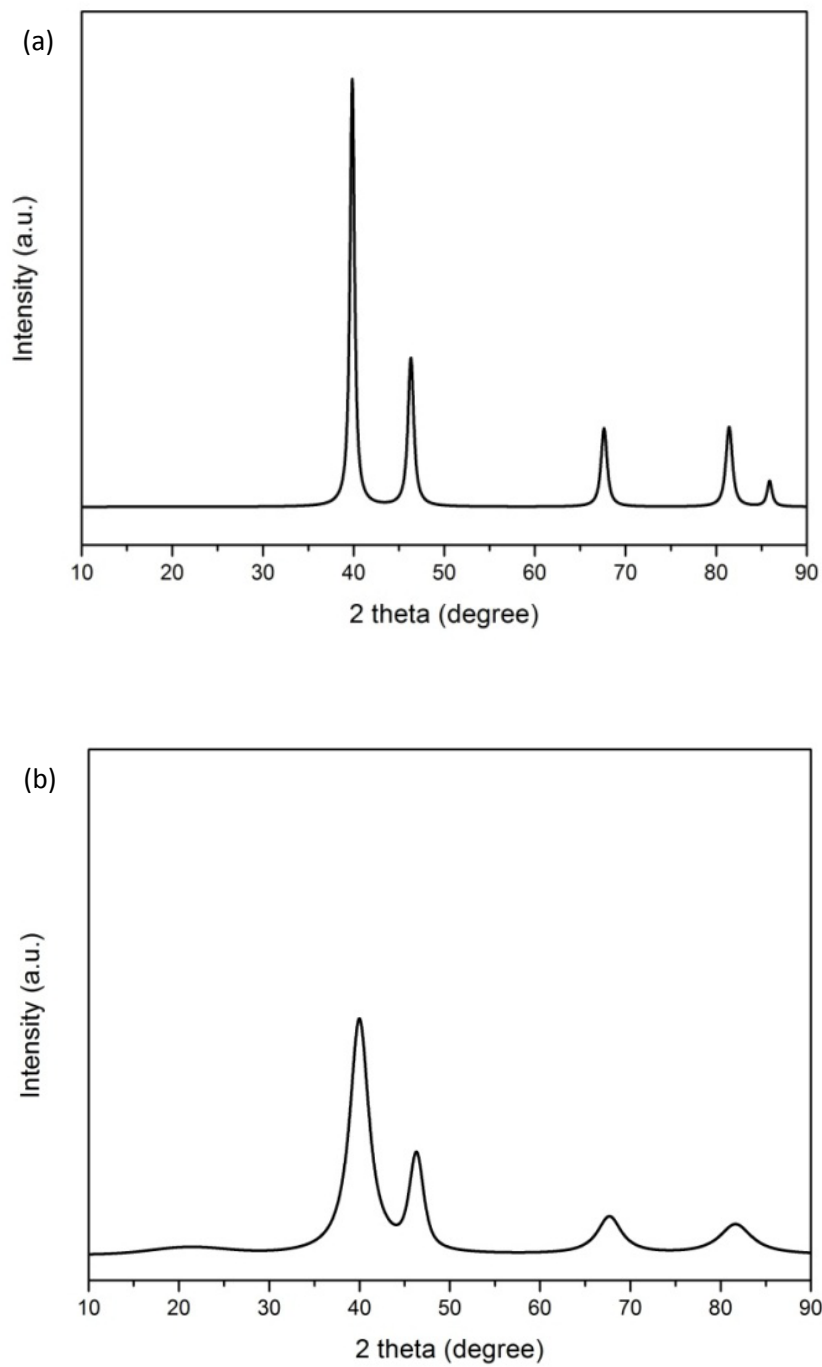


**Fig. S8** XRD spectra of Pt nanocrystals synthesized from reactions (a) without and (b) with the addition of OLA-GO.